

International Review of Electrical Engineering (IREE)

Contents

Editorial: A Message from the Editor-in-Chief <i>by Santolo MEO</i>	1
Modelling, Analysis and Control of DC-connected Wind Farms to Grid <i>by F. Iov, A. D. Hansen, P. Sørensen, F. Blaabjerg</i>	3
Modeling Ferrite Core Losses in Power Electronics <i>by A. Van den Bossche, V. C. Valchev</i>	14
Analysis of Non-Linear Inductors with the Use of Generalized Rayleigh Relations <i>by Z. Włodarski, A. Brykalski, J. Włodarska</i>	23
Winding Functions Theory and Maxwell's Equations Coupled Analytical Modeling of an Axial Flux PM Synchronous Machine <i>by N. Adbelkarim, J. Azzouzi, G. Barakat</i>	27
Adaptive Speed Observers for Sensorless Control of Induction Motors: a New Criterion of Stability <i>by E. Etien, N. Bensali, C. Chaigne, G. Champenois</i>	36
Stator Faults Diagnosis In Induction Machines <i>by S. Bachir, S. Tnani, G. Champenois</i>	44
Speed Synchronized Control of Permanent Magnet Synchronous Motors with Field-Weakening Capability <i>by L. Samaranayake, Y.K. Chin</i>	49
Linear Model and H^∞ Control of Shunt Active Power Filter <i>by T. Al Chaer, J.P. Gaubert, L. Rambault, C. Dewez</i>	57
Redundancy and Basic Switching Rules in Multilevel Converters <i>by Ó. López, J. Doral-Gandoy, C. M. Peñalver, J. Rey, F. D. Freijedo</i>	66
Characteristics and Comparison of Output Voltage Non-Idealities of Direct and Indirect Matrix Converters <i>by M. Jussila, M. Eskola, H. Tuusa</i>	74
A Novel Three-Phase UPS System with a Single-Phase Resonant HF Link <i>by M. K. Darwish</i>	83
A New Single Phase Single Stage High Frequency AC-DC Converter with Complex Programmable Logic Devices (CPLD) Controller <i>by S. Mekhilef, A. M. Omar, K. S. Muhammad</i>	90
A Tool for Phase Spectrum Retrieval from Impedance Amplitude Spectrum <i>by J. Ahola, E. Virtanen, T. Lindh, V. Särkimäki, R. Tiainen</i>	97
Frequency Converter Control in Single Field Programmable Gate Array Circuit <i>by O. Laakkonen, K. Rauma, A. Penttinen, T. Härkönen, J. Luukko, O. Pyrhönen</i>	104



A Novel Three-Phase UPS System with a Single-Phase Resonant HF Link

M. K. Darwish

Abstract – This paper presents a new three-phase uninterruptible power supply (UPS) system based on a single-phase resonant high frequency (HF) link and a single-phase transformer. The three-phase output voltage is constructed and regulated from a three-phase cycloconverter fed from the constant amplitude, constant frequency link voltage. The generation of a novel switching strategy for the three-phase cycloconverter is presented. The simulation of the proposed system is carried out and verified with experimental results. Copyright © 2006 Praise Worthy Prize - All right reserved.

Keywords: UPS, PWM converters, Resonant inverters, HF transformers

I. Introduction

In applications such as UPS and ac motor drives, three-phase inverters are commonly used to supply three-phase loads. It is possible to supply a three-phase load by means of three separate single-phase inverters [1], where each inverter produces an output displaced by 120° (of the fundamental frequency) with respect to each other. Though this arrangement may be preferable under certain conditions, it requires either a three-phase output transformer or separate access to each of the three phases of the load. In practice, such access is generally not available and requires large number of switching devices [2-6].

In previous publication [7], a single phase UPS output system based on resonant HF link and single transformer has been introduced. The block diagram is shown in Fig. 1. The resonant link offers high efficiency and small size heat-sink due to the reduction of the switching loss, snubberless operation, elimination of acoustic noise, low EMI problems and longer life of machine insulation (in case of drive system) due to low dv/dt . The HF link allows the isolation transformer to be designed at the link frequency rather than at the low output frequency so that its size and weight can be highly reduced. Moreover, the operation at HF link power conversion allows the minimization of the size of the output filter. The resonant inverter is switched at the carrier frequency such that a sinusoidal voltage of constant amplitude is produced across the resonant capacitor, and the inverter performs the zero-current switching thus reducing switch stresses, switching loss and EMI. This voltage is fed to the transformer's primary winding, where the transformer output voltage is applied to the cycloconverter to reconstruct the low-frequency output voltage. Since the input to the cycloconverter is of constant amplitude, the switching

angles of the cycloconverter have to be modulated, using a sinusoidal reference signal, in order to achieve a sinusoidal output voltage.

The single-phase configuration offers the output voltage to be controlled from the sinusoidal pulse-width modulation (SPWM) technique of the cycloconverter which has four bi-directional switches in full-bridge configuration. The system is so flexible that three-phase output voltages can be generated by adding another arm to the cycloconverter keeping the system with one resonant inverter and single-phase transformer. This configuration offers a compact three-phase UPS system which incorporates a single-phase resonant HF link and also a single-phase isolation transformer.

II. Circuit description

The detailed circuit diagram of the proposed dc-ac converter is shown in Fig. 2. The single-phase resonant HF link is established by a series resonant full-bridge inverter. The inverter-switches are switched in such a way that the output voltage (across the resonant capacitor) is a constant amplitude sine-wave at the link frequency. Although an ordinary square-wave inverter can be used in this configuration (using the same switching pattern), the resonant inverter is preferred in order to reduce the switching losses, switch stress, EMI and acoustic noise so that the system performance and efficiency can be improved. The inverter output voltage is applied to a single-phase transformer which provides the galvanic isolation and steps-up the voltage in order to obtain the required low-frequency fundamental component. Since the input to the cycloconverter is of constant amplitude, the switching angles of the cycloconverter-switches have to be modulated,

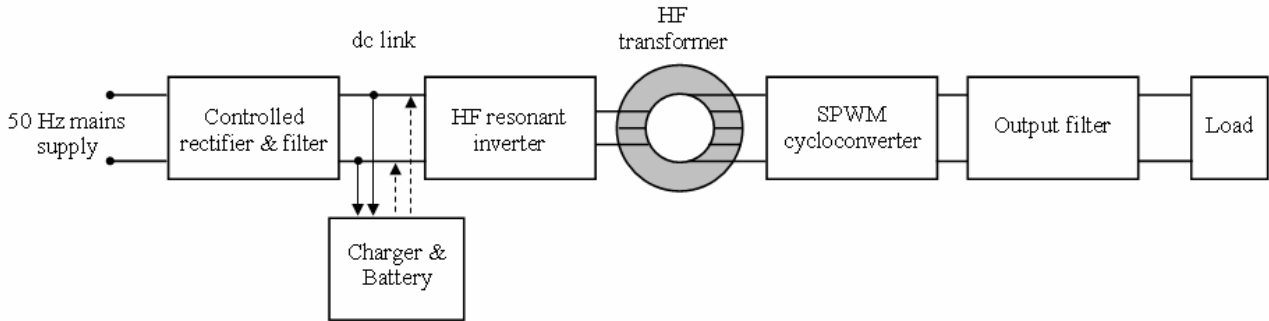


Fig. 1. Block diagram of the resonant HF link single-phase UPS system.

using sinusoidal reference signals, in order to achieve sinusoidal output voltages and hence the low-frequency three-phase output voltages can be regulated over a wide range of operation.

The three-phase cycloconverter consists of six bi-directional switches in full-bridge configuration. The bridge type bi-directional switch is preferred over the anti-parallel type bi-directional switch in order to reduce the overall number of the switching devices and simplify the control circuit despite the excessive voltage drop across the diodes. A three-phase LC output filter is required at the output terminals in order to suppress the associated harmonics.

III. Synthesizing the switching patterns

The objective of the three-phase SPWM cycloconverter is to shape and control the three-phase low-frequency output voltages in magnitude, frequency and phase with an essentially constant amplitude, constant frequency sine-wave input voltage.

To obtain a balanced three-phase sinusoidally-modulated voltages, a triangular wave at the carrier (link) frequency is compared with three sinusoidal control voltages that are 120° out of phase as shown in Fig. 3-a for a frequency modulation ratio (M_f) of 7. The resultant normalised three-phase line-to-line voltages (V_{AB} , V_{BC} , and V_{CA}) are shown in Figs. 3-b, c, d. The switching patterns of the resonant inverter is such that each diagonally opposite pair of switches (T_1 , T_4 , and T_3 , T_2) have a similar 50% duty ratio square-wave synchronised with the carrier triangular-wave as shown in Figs. 3-e, f. The normalised resonant inverter output voltage is shown in Fig. 3-g, where it is a constant amplitude sine-wave with a frequency equal to the carrier frequency and its state changes in the intervals defined by the peaks of the triangular carrier.

The switching patterns of the cycloconverter-switches GS_1-GS_6 can be synthesised in the following way: The individual pulses of the line voltage V_{AB} are alternately carried by the pair of switches S_1 , S_6 and S_3 , S_4 . While the pulses of V_{BC} are alternately carried by S_5 , S_6 and S_3 , S_2 and the pulses of V_{CA} are alternately carried by S_5 , S_1 . The pulses carried by the switching

pair S_1 , S_6 and S_3 , S_4 for the line voltage V_{AB} can be obtained by multiplying the line voltage V_{AB} by the normalised sine-wave of the inverter output as shown in Fig. 3-h. This step identifies the switching pulses of the pair of switches S_1 and S_6 ($GS_{1,6}$ – the positive pulses) and the switching pulses of the pair of switches S_3 and S_4 ($GS_{3,4}$ – the negative pulses). This step is repeated for the line voltages V_{BC} and V_{CA} . The total switching pattern of each switch can be obtained from ‘ORing’ the switching patterns accomplished by the same switch for different line voltages (for example; $GS_1 = GS_{1,6} \text{ OR } GS_{2,1}$). The final switching patterns of the cycloconverter-switches GS_1-GS_6 are shown in Figs. 3 (i-n).

It can be seen that all the switching patterns posses a half-wave symmetry where the switches in the same arm do not conduct at the same time to prevent short-circuiting the transformer output. Also, there are three switches which are turned-on at the same time (one from each arm), while there are some instants where all the six switches are turned-off. This switching strategy can be applied for any value of M_f (odd or even) and also not necessarily to be multiple of three (in order to eliminate the even harmonics) as required by the conventional switching strategies.

IV. Circuit Simulation

In order to verify the validity of the synthesized switching pattern, the dc-ac converter of the proposed configuration is simulated using the PSpice software. The dc link voltage is kept constant at 60V and the amplitude modulation index (M_a) is taken as 0.8, while the link frequency is taken as 1kHz in order to provide clear illustrating waveforms. The resonant frequency (f_r) of the inverter, where $f_r = 1 / (2\pi\sqrt{L_r C_r})$, is taken as $1.25 f_c$ (where f_c is the carrier frequency) in order to obtain a pure sine-wave voltage across the resonant capacitor [2].

Fig. 4 shows the simulated results of the resonant inverter output voltage, and the cycloconverter output voltage for one phase. The following points can be concluded from the harmonic spectra of the voltage waveform:

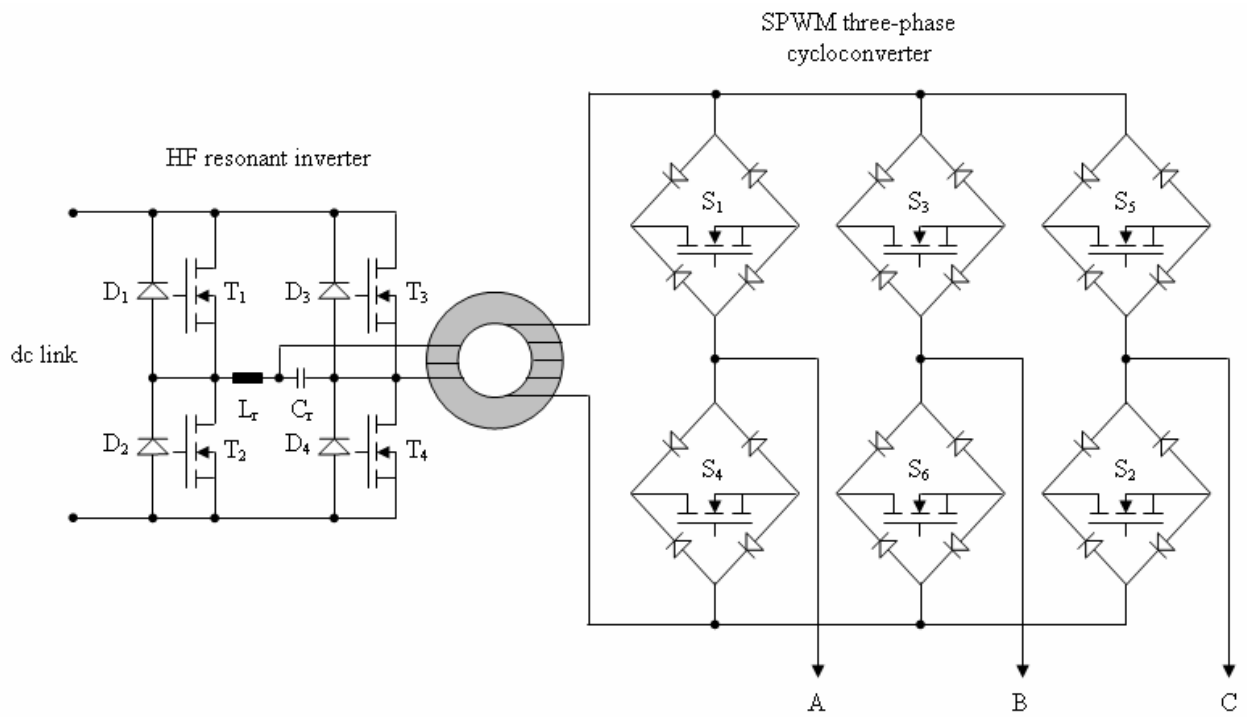


Fig. 2. Circuit diagram of the resonant HF link three-phase UPS system.

1. The phase voltages have the dominant harmonics at M_f, where only odd harmonics exist as sidebands, centred around M_f and its multiples, that is, M_f, 2M_f, 3M_f and so on. The harmonic spectrum can be expressed by the following equation:

$$H = j(M_f) \pm k \quad (1)$$

For odd values of j, the harmonics exist only for even values of k and, for even values of j, the harmonics exist only for odd values of k.

2. The dominant harmonics of the phase voltages (at M_f) are suppressed in the line voltage because they are 120° out of phase. The same argument applies to the suppression of the triplen sidebands of the associated harmonics in line voltages.
3. The proposed dc-ac converter is simulated for different values of M_f and M_a. It is found that the amplitudes of the harmonic components of the line voltages are almost independent of the value of M_f, although M_f defines the frequencies at which they occur. Table 1 presents the normalised harmonics (relative to the peak value of the resonant HF link voltage) as function of the amplitude modulation index (M_a).

TABLE I
NORMALISED HARMONICS OF THE LINE VOLTAGES

h	Ma				
	0.6	0.7	0.8	0.9	1.0
1	0.451	0.504	0.552	0.589	0.612
M _f ± 2	0.088	0.103	0.119	0.127	0.127
2M _f ± 1	0.300	0.297	0.288	0.273	0.261
2M _f ± 5	0.008	0.126	0.019	0.028	0.041
3M _f ± 2	0.142	0.140	0.128	0.108	0.094
3M _f ± 4	0.035	0.053	0.070	0.078	0.082
4M _f ± 1	0.047	0.009	0.018	0.022	0.027
4M _f ± 5	0.026	0.043	0.057	0.062	0.061
4M _f ± 7	0.006	0.009	0.018	0.026	0.030

During normal operation of the proposed configuration, the modulation index is kept constant at 0.8 such that the low-frequency fundamental component is 0.552 times the peak value of the link voltage. However, this modulation index will allow to increase under a closed-loop control during standby operation when the battery voltage starts to decrease.

For a link frequency of 20 kHz, the tank circuit comprises an inductor (L_r) of 80 μH and a capacitor (C_r) of 0.5 μF so that the peak value of the link voltage becomes 200V. Hence, the low-frequency (50Hz) output voltage will have a fundamental component of 110V. Since this component should be raised to 380√2V, a transformer turns-ratio of 4.88 is required. On the other hand, the voltage rating of the cycloconverter-switches will be raised to 976V.

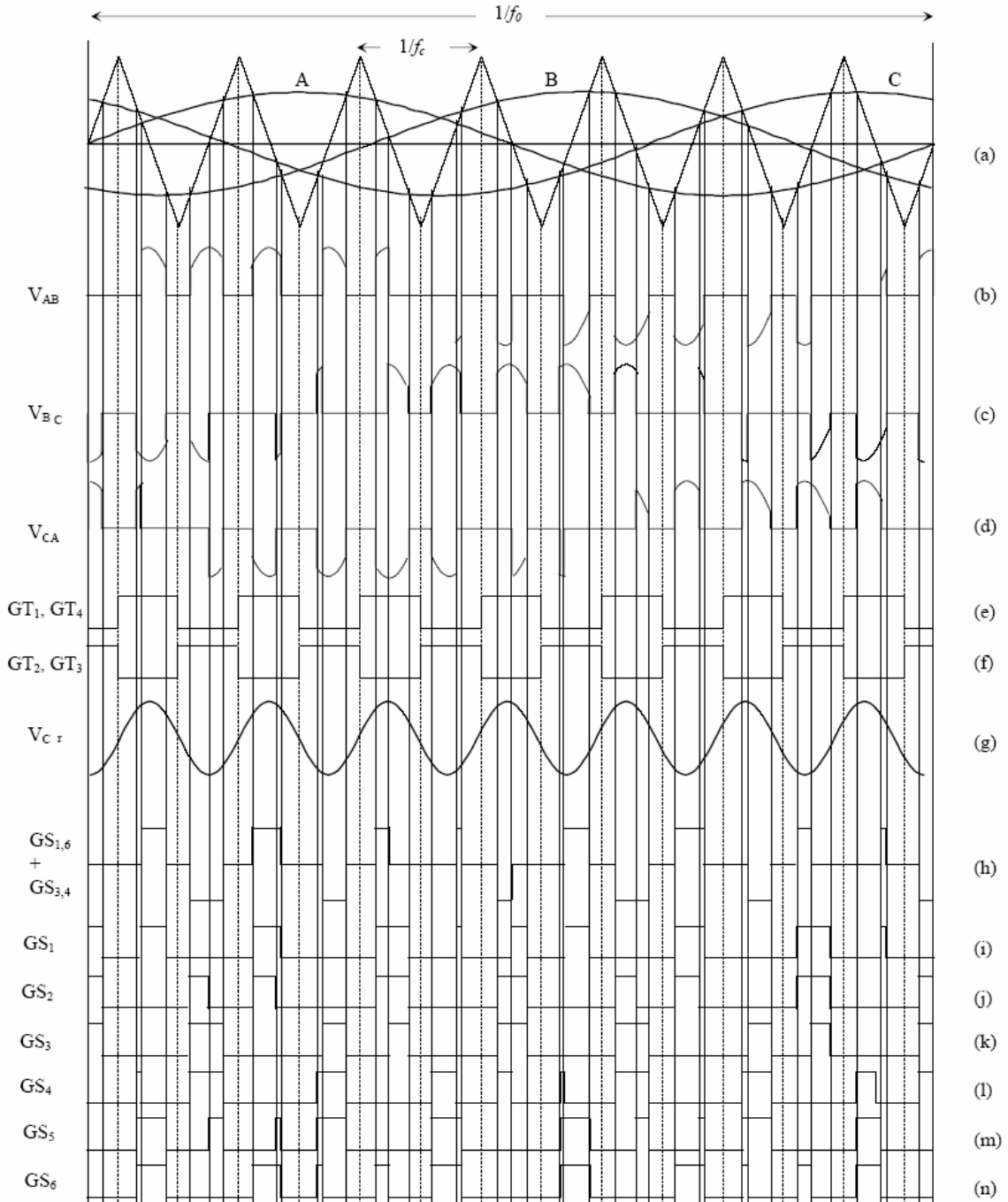


Fig. 3. Derivation of the switching patterns ($M_a=0.5, M_f=7$).

V. The HF Transformer Design

The choice of the link frequency depends on a compromise between size and efficiency. The size of the transformer, the inductor and filter capacitor can be greatly reduced by operating them at higher frequencies. However, switching losses and iron losses increase reducing overall circuit efficiency. For a constant flux density, the cross-sectional area of the transformer core is inversely proportional to the frequency.

So in theory, a 10 kHz transformer would require a core cross-sectional area 200 times smaller than the one operating at 50 Hz. In practice, the reduction can not be quite this large since the windings and insulation have to be capable of handling the same power rating. Furthermore, heat dissipation becomes a problem because of the reduced surface area. The overall reduction achieved in the size is 40% and in the weight is 39%. A further reduction will cause problems in the heat dissipation. Although almost any magnetic material

may be used for designing HF power transformer, ferrite cores are almost exclusively used in modern converter designs. Ferrite cores may not have very high operating flux density (most ferrites have a saturation flux density ranging from 0.3 to 0.5 T) but they offer low core losses at high frequencies. Ferrite materials are relatively poor conductors of heat and due to manufacturing problems are limited in size to a core sectional area about 30mm². Amorphous materials are worth noting. At present, they are rather expensive and have the reputation of being fragile. They have much lower losses than the traditional grain oriented silicon steel and ferrites, at similar levels of the flux. Recently, they were used for utility distribution transformers where no-load losses are of paramount importance and may well in the future provide a bridge for the power-electronics designers between low-frequency conventional and HF ferrite cores. Amorphous metals are a group of alloys with metallic properties but without the crystalline lattice structure of conventional metals. They have no atomic order such that hysteresis is negligible. The transformer used through this work was a toroidal strip-wound core, cobalt base, Metglas alloy 6030F [8]. According to the core loss data of this core [8], the following equation for the core loss per unit volume, P_{co} , is synthesized:

$$P_{co} = 0.9 f_s^{1.8} B_m^2 K_s \cdot 10^{-8} \text{ Watts/cm}^3 \quad (2)$$

where, f_s is the link frequency (Hz), B_m is the maximum flux density (Gauss) and K_s is the core loss temperature coefficient.

In order to minimise the size of the HF transformer, an optimum ratio of copper loss to core loss has been driven. It is found that this ratio is generally equal to half the index of the maximum flux density in (2), which results in equal losses for this material. A computer aided transformer design procedure is used to find the smallest core from the available list of the Metglas alloy 6030F. For a 1kVA capacity and a link frequency of 20kHz, the theoretical efficiency is found to be 99% during both modes of operation of the proposed UPS configuration.

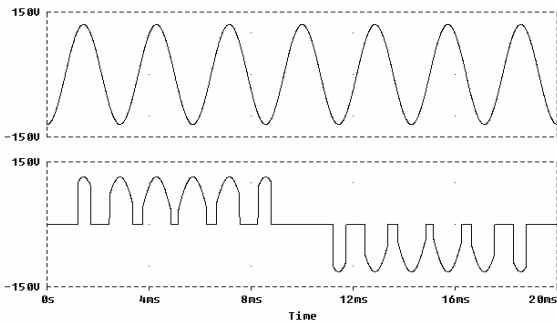


Fig. 4. Simulated results of the output voltage and HF link.

VI. Experimental results

A prototype UPS system with a HF transformer having a unity turns-ratio and a link frequency of 20kHz ($M_f = 400$) was built to verify the feasibility of the proposed configuration. The switching patterns required by the system converters are generated using custom hardware. Also, an SDK-86 microcomputer system is used to provide the supervisory control and monitoring functions. The system parameters (some shown in tables 2 & 3) such as mains voltage, output voltage and current, battery voltage, internal temperature and manual interrupt request are put under continuous monitoring such that the microprocessor can switch between the normal and standby modes of operation and, at the same time, provides a continuous visual status of the system on a fabricated control panel.

TABLE 2
SYSTEM PARAMETERS USED IN THE EXPERIMENTAL RESULTS

V _d	M _a	M _f	L _r	C _r	η
60	0.8	400	2.2 mH	60 μF	85%

TABLE 3
THE SPECIFICATIONS OF THE USED HF TRANSFORMER

N ₁ = N ₂ = N ₃	A _s	B _m	P _{cu}
19	38 cm ²	4488 G	1.2 W

One of the output line voltages and the resonant HF link voltage are shown in Fig. 5. Their corresponding harmonic spectra are shown in Figs. 6 and 7. The HF link voltages has only a fundamental component of 200V at 20kHz since it is a pure sinewave. The output voltages have their fundamental component of 110V at 50Hz and the dominant harmonics appear as sidebands of M_f and $2M_f$ respectively. The proposed UPS system has been tested for mains failure conditions as shown in Fig. 8, where the oscillogram shows the single-phase mains voltage and one of the output line voltages. It can be seen that the load voltage is not affected by the condition of the mains voltage. Identical results were obtained at the mains recovery conditions.

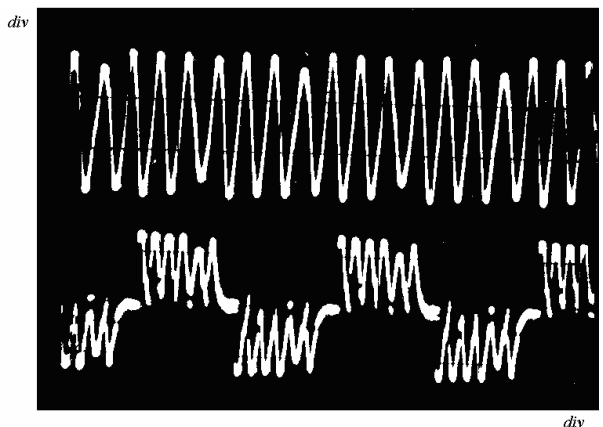


Fig. 5. Experimental results of the HF link (upper curve) and output voltage (lower curve) - (5 ms/div, 100 V/div)

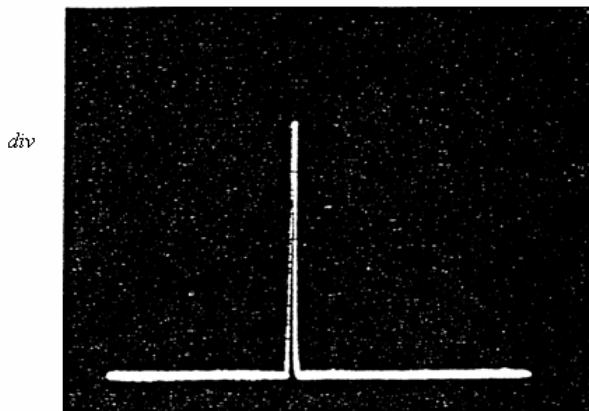


Fig. 6. Harmonic spectrum of the HF link voltage.
(20 V/div)

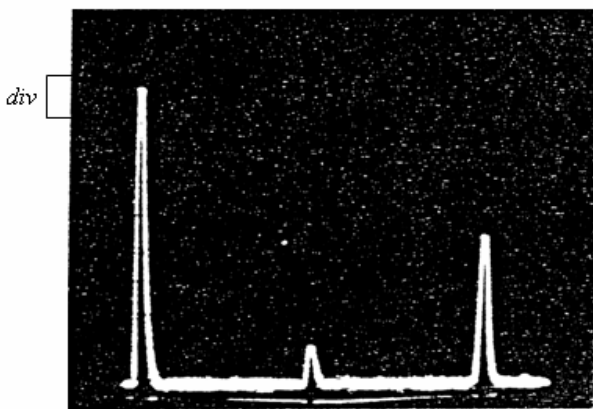


Fig. 7. Harmonic spectrum of the output line voltages.
(20 V/div)

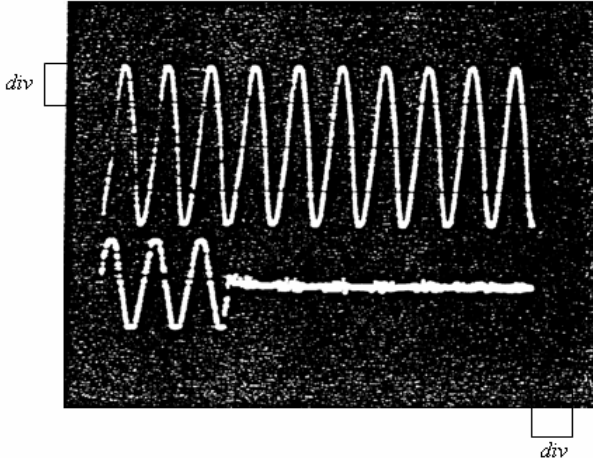


Fig. 8. UPS performance during mains failure.
(20 ms/div, 100 V/div)

The three-phase output line voltages after the connection of the output filter for a resistive load are shown in Fig. 9. These voltages are connected in response to the three-phase sinusoidal reference voltages. A photo of the tested experimental system is shown in Fig. 10.

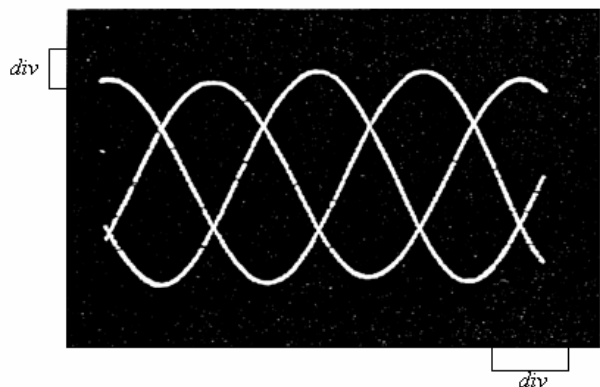


Fig. 9. The three-phase output line voltages.
(5 ms/div, 100 V/div)

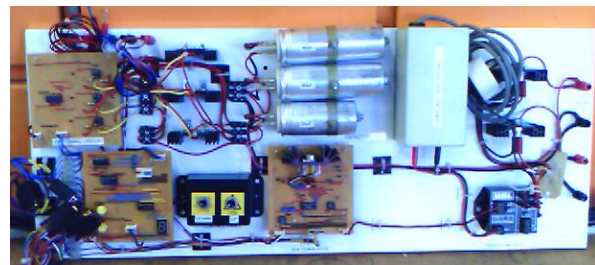


Fig. 10. The tested experimental system.

VII. Conclusions

A novel on-line resonant HF link three-phase UPS system, which has been supplied from a single-phase mains supply, has been developed. The system has a resonant single-phase HF link and a single-phase isolation transformer. A balanced three-phase output voltage is obtained from a cycloconverter which has six bi-directional switches in full-bridge configuration and fed from the constant amplitude constant frequency single-phase resonant HF link. The output voltage is controlled from the SPWM technique used by the cycloconverter. The isolation transformer is designed to operate at the link frequency. The output phase voltages have their dominant harmonics at the carrier frequency while the line voltages have their dominant harmonics at double the link frequency. The simulation and experimental results are found in close agreement and the system performance during the mains failure and recovery conditions is highly acceptable. The introduced configuration is expected to reduce the size and weight of conventional three-phase UPS systems by about 40%.

References

- [1] I. Ando, I. Takahashi, Y. Tanaka, and M. Ikchura, Development of high efficiency UPS having active filter ability composed of a three arms bridge, *Proceedings of 23rd International Industrial Electronics, Control and Instrumentation*, pp. 804-809, 1997.
- [2] S. B. Bekiarov, and A. Emadi, Uninterruptible power supplies: classification, operation, dynamics, and control, *Proceedings of*

- the 17th IEEE Applied Power Electronics Conference*, pp. 597-604, March 2002.
- [3] B. K. Lee, B. Fahimi, and M. Ehsani, Overview of reduced parts converter topologies for AC motor drives, *Proceedings of the 32nd Power Electronics Specialists Conference*, pp. 2019-2024, 2001.
- [4] G. J. Su, Design and analysis of a low cost, high performance single-phase UPS system, *Proceedings of the 16th IEEE Applied Power Electronics Conference*, pp. 597-604, 2001.
- [5] A. Emadi, Uninterruptible power supplies and active filters, CRC Press, 2005
- [6] R. Krishnan and S. Srinivasan, Topologies for Uninterruptible Power Supplies, *IEEE Inter. Symposium on Ind. Elect.*, Vol. IA-19, pp. 122-127, 1993.
- [7] T. Abdelhamid, M. K. Darwish, P. Mehta, A. Mohamadein, M. Abo-Elela, A new flexible and compact high frequency link online UPS system, *European Power Electronics Journal*, Vol. 5, no. 2, pp. 9-14, 1995.
- [8] VACUUMSCHMELZE GMBH & Co.N., <http://www.allstarmagnetics.com/VAC/vitrovacISDNcore.s.pdf>. Accessed October 2005.

Author's informations



Mohamed K. Darwish (IEE Member 89–CEng 90) was born in Alexandria, Egypt in 1955. He received the BSc degree in Electrical Engineering from Helwan University, Cairo, Egypt, and the PhD degree from Brunel University in 1978 and 1987 respectively. Since 1987 he is a lecturer in Power Electronics at Brunel University and since 1995 he is the Power Electronics group leader.

His research interests include active filtering techniques, UPS systems and Power Quality issues. Dr. Darwish has published over 70 papers in leading journals and conferences.

***International Review of
Electrical Engineering
(IREE)***

Authors

	pag.		pag.
Adbelkarim N.	<u>27</u>	Lindh T.	<u>97</u>
Ahola J.	<u>97</u>	López Ó.	<u>66</u>
Al Chaer T.	<u>57</u>	Luukko J.	<u>104</u>
Azzouzi J.	<u>27</u>	Mekhilef S.	<u>90</u>
Bachir S.	<u>44</u>	Muhammad K. S.	<u>90</u>
Barakat G.	<u>27</u>	Omar A. M.	<u>90</u>
Bensiali N.	<u>36</u>	Peñalver C. M.	<u>66</u>
Blaabjerg F.	<u>3</u>	Penttinen A.	<u>104</u>
Brykalski A.	<u>23</u>	Pyrhönen O.	<u>104</u>
Chaigne C.	<u>36</u>	Rambault L.	<u>57</u>
Champenois G.	<u>36, 44</u>	Räuma K.	<u>104</u>
Chin Y.K.	<u>49</u>	Rey J.	<u>66</u>
Darwish M. K.	<u>83</u>	Samaranayake L.	<u>49</u>
Deweze C.	<u>57</u>	Särkimäki V.	<u>97</u>
Doval-Gandoy J.	<u>66</u>	Sørensen P.	<u>3</u>
Eskola M.	<u>74</u>	Tiainen R.	<u>97</u>
Etien E.	<u>36</u>	Tnani S.	<u>44</u>
Freijedo F. D.	<u>66</u>	Tuusa H.	<u>74</u>
Gaubert J.P.	<u>57</u>	Valchev V. C.	<u>14</u>
Hansen A. D.	<u>3</u>	Van den Bossche A.	<u>14</u>
Härkönen T.	<u>104</u>	Vartiainen E.	<u>97</u>
Iov F.	<u>3</u>	Włodarska J.	<u>23</u>
Jussila M.	<u>74</u>	Włodarski Z.	<u>23</u>
Laakkonen O.	<u>104</u>		